PNL-SA-7718
CONF-790838--3

THE DEVELOPMENT OF NOMARSKI MICROSCOPY FOR QUANTITATIVE DETERMINATION OF SURFACE TOPOGRAPHY[a]

J. S. Hartman
R. L. Gordon
D. L. Lessor

Pacific Northwest Laboratory[b]
Richland, Washington 99352

ABSTRACT

The use of Nomarski differential interference contrast (DIC) microscopy has been extended to provide nondestructive, quantitative analysis of a sample's surface topography. Theoretical modeling has determined the dependence of the image intensity on the microscope's optical components, the sample's optical properties, and the sample's surface orientation relative to the microscope. Results include expressions to allow the inversion of image intensity data to determine sample surface slopes.

A commercial Nomarski system has been modified and characterized to allow the evaluation of the optical model. Data have been recorded with smooth, planar samples that verify the theoretical predictions.

(a) Prepared for the U.S. Department of Energy, Division of Basic Energy Sciences, under Contract EY-76-C-06-1830.
(b) Operated by Battelle Memorial Institute.

DISCLAIMER

I. INTRODUCTION

The development of a nondestructive technique for evaluation of the surface topography of reflective samples would be useful for experimental studies in many technical areas. Surface topography of laser mirrors is critical for breakdown and damage phenomina in high powered laser systems. Mirror topography is also a key source of optical scattering in laser and solar energy systems. Studies of basic friction mechanisms also require a knowledge of the topography of the two sliding surfaces. But nondestructive techniques have not been readily available to obtain quantitative data from relatively smooth surfaces.

Nomarski differential interference contrast (DIC) microscopy has long been recognized for its extremely useful revelations of the qualitative nature of the variations in surface heights for reflective specimens.[1,2] Bertocci and Noggle used the technique to measure slopes on large metallographic specimens by an iterative procedure,[3] and the present authors have presented a theoretical analysis of Nomarski DIC microscopy which indicated the possibility of using the continuum of intensity values in the DIC image for obtaining surface topographical information.[4] That theory resulted in expressions for the dependence of intensity on the optical components and their relative orientations, the sample's slope and optical properties, and the orientation of sample slopes with respect to a reference direction defined by elements required for DIC image formation.

This discussion begins with a verbal description of the operation of Nomarski reflection microscopy and then presents the salient features of the above-mentioned theoretical analysis. Modifications of a commercially available microscope to permit quantitative opration is then described. An alignment procedure, methods of calibration, and results of experiments which permit the determination of the slope of tilted planar samples from measurements of intensity in the image plane are detailed.

II. OPERATING PRINCIPLES OF NOMARSKI MICROSCOPY

Image formation in Nomarski differential interference contrast (DIC) microscopy is the result of the interference of two distinct beams that reach the image plane. Nomarski reflection microscopy uses polarized input light, a birefringent prism, and a second polarizer to analyze the output light and produce a DIC image. The geometrical arrangement of the optical elements is shown in Fig. 1. Proper alignment of these elements produces two orthogonally polarized beams incident on the sample with a relative displacement comparable to the resolution limit of the objective. Image formation can best be understood by considering an experiment with a reflecting surface whose normal is parallel to the optical axis vertical of the microscope. The two polarization components of rays moving toward the sample experience relative phase shifts which depend on their positions as they pass through the prism. If an interference image were to be formed with these beams the observer would see a nonuniform intensity and interference fringes. But in reflection microscopy the horizontal sample causes the return path for each ray to be on the opposite side of and at an equal distance from the microscope optical axis. The second passage through the prism again results in unequal phase changes across the prism. But the side-to-side positional exchange by the incident and reflected rays causes differences in relative phase shift across the image to cancel. The system is therefore self-compensating. The double pass through the prism results in a single value for relative phase shift across the entire image. The image is thus formed within one inference fringe. In the absence of surface asperities the image is of uniform intensity, but variations in the sample's surface slope cause local variations in the angle of incidence and hence the angle of reflection. Rays from asperities thus strike the prism at positions and angles determined by the surface topography and result in additional relative phase differences which act to modulate the intensity distribution in the resulting image.

Collimated monochromatic light should be used to form the input beam. Use of uncollimated light results in nonuniform compensation and introduces random spatial changes of intensity which are unrelated to surface topography

of the sample. The use of monochromatic light, in contrast to broad-band illumination, provides enhanced sharpness for interference fringes and yields better definition of asperity-related intensity changes in the image.

The critical element in the system is the Nomarski prism, a Wollaston prism as modified by Nomarski. The prism is made with two wedges of birefringent material which are cut and assembled in a manner which splits an incoming beam into two components (orthogonal polarizations) which intersect after exiting the prism. Intersections of the exiting beams occur in a plane which will be referred to as the "plane of apparent splitting." The prism geometry and "plane of apparent splitting" are illustrated in Fig. 1a. The prism is oriented in the system so the plane of apparent splitting is perpendicular to the optical axis of the microscope. It should be noted that the prism not only splits the two polarization components but also causes a relative phase shift between them. The amount of relative phase shift between the beams varies linearly with motion of the input beam along the prism shear direction.[4] Translation of the prism along the shear direction, i.e., the direction of relative displacement between the two emergent beams, allows adjustment of the phase difference between the beams and therefore the average intensity in the DIC image.

The objective lens is located one focal length beyond the plane of apparent splitting. This causes the two beams passing through that plane at different angles to be focused by the objective lens at different positions near the sample's surface in the back focal plane of the objective (Fig. 1b). As indicated in Fig. 2a the beams reflected from the sample are then recombined into a single beam by the prism on the return path.

Next examine the function of the polarizer and analyzer and the overall system operation. The polarizer is used to adjust the beam polarization incident on the Nomarski prism permitting direct control over the relative amplitude of the two split beams leaving the prism and incident on the sample's surface. Quantitative surface measurements require adjustment of the polarizer to yield two beams of equal amplitude at the sample.

The analyzer is necessary for DIC image formation. The beam preceding the analyzer is composed of two orthogonally polarized, co-linear beams which

cannot interfere. The analyzer passes a common polarization component from each beam which allows their interference and the formation of the DIC image in the microscope eyepiece or at the film plane.

It should be noted that the linear motion indicated for the Nomarski prism in Fig. 1 may not be the standard motion available for a given commercial instrument but has been indicated here due to its importance in maintaining constant shearing direction and equal intensities in the two beams throughout the range of prism travel.

A theoretical model has been developed[4] which embodies these operating principles and explicitly includes effects of the optical elements and the optical properties of the sample. The model describes the dependence of the image intensity on the relative phase change between beam components and yields expressions for that relative phase change. The image intensity can be written

$$I = I_o \, [C + D(1 - \cos X)] \tag{1}$$

$$= I_{max} \, [Q + 1/2(1-Q)(1 - \cos X)] \tag{2}$$

where

$$C = \cos^2 (A-P) + \varepsilon \sin 2(A-P) + \varepsilon^2 \sin^2 (A-P), \tag{3}$$

$$D = - \sin 2A \; 1/2(1 - \varepsilon^2) \sin 2P + \varepsilon \cos 2P \; . \tag{4}$$

Here A and P are the angles made by the analyzer pass direction and the polarizer pass direction, with the shear direction and ε is the relative amount of the attenuated polarization component passed by the polarizer or analyzer.

I_{max} is the maximum image intensity and occurs when $\cos X = -1$. Hence

$$I_{max} = I \, (C + 2D), \tag{5}$$

$$Q = C/(C + 2D). \tag{6}$$

"Ideal" optics ($\epsilon = 0$), with $P = 45^\circ$ and $A = 135^\circ$ result in $C = 0$ and $Q = 0$. Departures from ideal optics tend to give intensity relations of the form of Eq. (2) with nonzero Q, as can be substantiated experimentally by adjusting the Nomarski prism to vary the phase shift X and observing that the minimum intensity is not zero. The form of Eq. (2) is probably more general than the assumptions for which it was derived, namely, that nonzero Q comes from departures from $P = 45^\circ$, $A = 135^\circ$, $\epsilon = 0$, or from an equivalent ideal set of these parameters. Finite band width and departures from small angle approximations might contribute to nonzero Q, but in a forthcoming experimental paper we will report good agreement with Eq. (2) with an experimental 70-fold reduction of intensity from I_{max} to minimum intensity $I_{min} = Q\ I_{max}$.

The model was developed using geomtrical optics and results were confirmed by comparison with those obtained using the Eikonal equation. Application of the model requires accurate knowledge of the relative phase differences and their dependence on the system optics and the sample. The utility of the technique for surface analysis is ultimately based on the separability of effects on phase shift due to sample geometry from those due to prism position. This is seen in the expression for the total relative phase shift,

$$X = \alpha + \beta \tag{7}$$

where α is related to the sample topography and β is governed by the prism position. Expressions for both contributions to the total phase shift were developed for an optical system which allowed the linear translation of the prism along its shear direction. The prism retardation is then a linear function of the prism position.

$$\beta = \beta_0 + x \frac{d\beta}{dx} \tag{8}$$

where x is the wedge position, β_0 is the retardation at x=0, and $\frac{d\beta}{dx}$ is the rate of phase change with changing prism position. The prism position is

measured relative to an arbitrary reference. If that reference is changed, the value of β_o changes accordingly. But $\frac{d\beta}{dx}$ remains constant and depends only on the properties of the birefringent prism and the illuminating wavelength (λ),

$$\frac{d\beta}{dx} = \pm \frac{8\pi}{\lambda} \left(n_e - n_o\right) \tan \theta_w, \tag{9}$$

where $n_e(n_o)$ is the extraordinary (ordinary) refractive index of the prism material and θ_w is the common wedge angle of the two halves of the Nomarski prism. The sign ($\pm$) is determined by the Nomarski prism orientation (i.e., prism inversion changes the sign). The remaining phase shift (α) is then governed by the surface geometry and constants of the optical system. For the sample geometry seen in Fig. 3:

$$\alpha = -\frac{1}{2} f \tan 2\psi \cos \phi \frac{d\beta}{dx} \tag{10}$$

Where f = objective focal length, ψ = surface slope angle, and ϕ = angle between the prism shear direction and the surface "fall line."

III. EXPERIMENTAL SYSTEM

A. DESCRIPTION

The microscope system used in this study was a Zeiss Ultraphot II.[a] The microscope was equipped with an adjustable polarizer (0 to 90°), an adjustable analyzer (0 to 180°), and a narrow bandpass color filter (10 nanometers half bandwidth) with a center wavelength of 545.0 nanometers.

The Nomarski prism assembly was modified from the Zeiss configuration to provide prism motion parallel to the prism shear direction using a dovetail slide with a micrometer screw drive providing a resolution of 0.0001 in. (Fig. 4). This allowed adjustment of the beam position on the prism, permitting adjustment of the relative prism retardation while maintaining fixed angular orientations between the optical elements in the microscope.

Samples were mounted on a goniometer head equipped with adjustment screws on its base to allow complete control of the orientation of the sample surface with respect to the microscope optical axis. The sample assembly was placed on a rotating sample stage available with the microscope. The stage permitted independent rotation of the sample about the optical axis of the microscope.

Image intensities were measured with an EGG Model 550-2 photodetector mounted in the film plane of the microscope. Measured intensities were thus average values and not related to effects of small asperities. System evaluation was accomplished using large (1.52 in. dia), super smooth (10-20 Å rms roughness) mirrors. The photodetector will be replaced by film for investigation of small features.

B. OPTICAL ALIGNMENT

System characterization must be preceded by an alignment procedure, the object of which is to set the polarizer to pass equal intensities along each

(a) Reference to a company or product name does not imply approval or recommendation of the product by the Pacific Northwest Laboratory or the U.S. Department of Energy to the exclusion of others that may be suitable.

of the orthogonal optical axes in the Nomarski prism (parallel and perpendicular to the prism shear direction). The analyzer is then set orthogonal to the polarizer.

The first step in alignment is to locate the optical axes of the Nomarski prism. The procedure is based on the fact that plane polarized light will pass unaltered through a birefringent crystal only when the plane of polarization coincides with one of the optical axes. The alignment steps thus determine the direction of the prism optical axes by iteratively finding the relative settings of polarizer, analyzer, and the Nomarski prism which yield an extinguished output beam.

The procedure requires a flat mirror mounted on the sample stage orthogonal to the microscope optical axis, a Nomarski objective assembly including an objective lens and a Nomarski prism with linear prism travel, a standard objective lens with the same magnification as the Nomarski objective, and a narrow band color filter on the microscope light source. The procedure consists of the nine steps shown in Table I. The first five serve to accurately determine the angular locations of the optical axes in the Nomarski prism by an iterative search. The last four steps then set the polarizer and analyzer for quantitative system operation. The procedure will produce equal intensities of light polarized along each of the orthogonal axes of the Nomarski prism. The final configuration of optical elements leaves the polarizer and analyzer aligned orthogonally with the polarizer set at 45° to the optical axes of the Nomarski prism.

TABLE I.

Step 1. Install the standard objective lens.

Step 2. Adjust the polarizer and analyzer for extinction.

Step 3. Remove the standard objective lens and install the Nomarski objective assembly.

Step 4. If the output beam is still extinguished, record the directions of the rotatable polarizer and analyzer. This will occur only when the polarizer and analyzer are parallel to the prism optical axes.

Step 5. If the output beam is not extinguished, rotate the analyzer a small amount and repeat steps 1-5.

Step 6. Rotate polarizer 45° from the final setting obtained in Step 4. RECORD polarizer setting.

Step 7. Install standard objective lens.

Step 8. Adjust analyzer for extinction with the new polarizer position. RECORD the analyzer setting.

Step 9. Install the Nomarski objective assembly.

C. CALIBRATION

The separability of the phase shift introduced by the Nomarski prism from that produced by variations in surface height on the sample permits the calibration required for obtaining quantitative topographical results. Calibration is based on Equations (2, 7, and 8). Examination of Equation (2) reveals the maximum and minimum measured intensity are simply I_{max} and

$$I_{min} = I_{max} Q \tag{11}$$

If we further define

$$I' = I_{max}(1 - Q), \tag{12}$$

the intensity of Eq. (2) can easily be seen to consist of a constant background resulting from optical leakage plus a contribution which is modulated by the total relative phase shift X.

$$I = I_{min} + I'(1 - \cos \chi)/2 \tag{13}$$

For the special case when a flat sample is orthogonal to the microscope optical axis, $\alpha = 0$ and the intensity can be written as

$$I = I_{min} + I' \left[1 - \cos \left(\beta_o + x \frac{d\beta}{dx}\right)\right]/2 \tag{14}$$

Eq. (14) is the basis for instrument calibration. With a flat sample mounted orthogonal to the optical axis of the microscope, translation of the prism across the field of the objective produced a changing image intensity, $I(x)$, which is dependent on prism position. The leakage parameter Q can be obtained from

$$Q = I_{min}/I_{max}, \tag{15}$$

and the parameter I' can then be found using Eq. (12). The intercept β_o and the slope $d\beta/dx$ of Eq. (8) can be obtained either by using nonlinear regression to directly compare $I(x)$ to the model of Eq. (14), or by inverting that equation to obtain the argument of the cosine function,

$$\beta(x) = \cos^{-1} \left[1 - 2\, I(x) - I_{min}\right]/I' \ . \tag{16}$$

Standard linear regression of the arc-cosine in Eq. (16) on prism position x then yields least-squares estimate of the slope and intercept of Eq. (8).

Determination of system parameters was carried out using a flat, super smooth mirror and average intensities measured with the photometer mounted as described above. Visual examination of the Nomarski image showed uniform illumination and no significant discrete defects. The sample was oriented with its surface orthogonal to the microscope optical axis ($\psi = 0 \rightarrow \alpha = 0$) to allow independent assessment of the prism retardation, β, in Eq. (7).

Image intensity data were then recorded as a function of prism position as the prism was translated through its entire range of 0.175 in. (0.445 cm).

Intensities were recorded at prism position intervals of 0.001 in. The data points shown in Fig. 5a demonstrate the sinusoidal dependence on the prism position predicted by Eq. (14).

The data were analyzed using both linear and nonlinear regression. Linear regression using Eq. (16) only provides information on the dependence of phase retardation on prism position. Fig. 5b shows the results of the application of this analysis to the raw data similar to that in Fig. 5a. Estimates of the quantities β_0 and $d\beta/dx$ correspond to the intercept and slope of the line in Fig. 5b. The resulting values provide a complete description of prism retardation as given in Eq. (8).

Nonlinear regression was used to estimate both the prism parameters (β_0 and $d\beta/dx$) and the experimental intensity parameters (I_{max} and Q) by comparing Eq. (2) to the raw data. In the comparison, Eq. (8) was used for the total phase shift X. All nonlinear regression calculations were conducted using the FORTRAN program, NLIN, based on an algorithm due to Marquardt[5] and adapted to run on a PDP11/10 minicomputer.

Table II compares the results of linear and nonlinear regression for a 40X Nomarski objective.

Table III lists the results of nonlinear regression fits to the data, while the continuous curve in Fig. 5a is typical of the agreement between experiment (points) and the calculated function for the 40X objective. The estimates are highly reproducible as evidenced by the standard deviations listed in Table III.

Comparison of Tables II and III reveals uniformly good agreement between linear and nonlinear regression for $d\beta/dx$ but a large difference in the intercept, β_0. The difference was a result of the disassembly of the 40X objective assembly between experiments and a subsequent change in the zero setting of the micrometer relative to the microscope. This caused the change in the value of β_0 but did not alter the value of $d\beta/dx$ which is controlled by the physical constants of the Nomarski prism, Eq. (2).

TABLE II. Comparison of Results from Linear and Nonlinear Regression

Assembly	Method	B_o [(a)], Rad.	dβ/dx, Rad./in.
40X	Linear	16.0103 ± 0.0158	-40.7126 ± 0.0491
	Nonlinear	15.9604	-40.5731

(a) Value is not absolute. Addition of $2n\pi$ leaves results unchanged.

TABLE III. Results of Translation Experiments
40X Objective

Set	β_o	dβ/dx, $in.^{-1}$	I_o	Q	SE[(c)]
1[(a)]	7.520	-40.506	1.727	0.00911	0.523E-02
4[(a)]	7.494	-40.445	1.716	0.00874	0.467E-02
5E[(b)]	7.529	-40.558	1.785	0.00857	0.698E-02
5O[(b)]	7.527	-40.554	1.785	0.00866	0.689E-02
AVG.	7.518	-40.516	1.754	0.009	
ST. DEV.	0.016	0.053	0.037	0.0002	
%	0.214	0.13	2.11	2.68	

(a) Resolution = 0.005 in.
(b) E(O) stands for Even (Odd) points of the set. Resolution = 0.001 in.
(c) Standard error of estimate.

Uncertainty in the leakage parameter Q is indicative of the reproducibility of the alignment procedure. The extremely small value of Q makes its determination sensitive to fluctuation in the photometer readings due to noise and changes in background illumination. It can be seen from Table III that conditions for the three translation experiments using the 40X objective were highly reproducible with the standard deviation of Q amounting to only 2.68%.

IV. MEASUREMENT OF SURFACE SLOPES

Results of experiments to determine surface slopes from intensity data obtained with a flat sample whose surface normal makes an angle ψ with the microscope optical axis will now be presented. With the prism at a fixed position x_o, the total phase X can be written

$$\psi = \beta(x_o) - \left[\frac{f}{2} \tan 2\psi \cos \phi \frac{d\beta}{dx}\right] \tag{17}$$

In Eq. (17), $\beta(x_o)$ represents the constant prism retardation at the position x_o, and ϕ is the angle between the surface fall line and the shearing direction of the prism. The total phase thus contains a constant term and a sinusoidal term in ϕ whose amplitude is governed by the sample's surface slope ψ. From Fig. 5a, it is seen that the value of x_o determines the nominal operating intensity while the oscillating phase component causes intensity modulation. For quantitative surface evaluations it is desirable to select $\beta(x_o) = \left(\frac{2n+1}{2}\right)\pi$ which corresponds to a mid-range image intensity for a zero slope sample. This operating point provides a linear relationship between intensity modulation and small surface slopes. It also allows the direct determination of surface slope sign (+ or -) from the measured intensity changes due to the single valued nature of the curve between each adjacent maximum and minimum. Figure 6 illustrates the predicted effective surface slope range for three Nomarski objective assemblies.

Numerical values of surface slopes were determined using rotational intensity data ($I(x_o, \phi)$ vs. ϕ) and nonlinear regression analysis. The flat copper sample was tilted on the goniometer to a series of angles less than 4°. The maximum tilt angle was governed by mechanical interference of the sample surface and the objective lens housing. Data were recorded at 5° intervals ($\Delta\phi$) using the modified 40X Nomarski objective assembly. The prism setting of 0.3785 in. produced a prism retardation of 7.818 radians, corresponding to a principal value of 0.489π radians. This resulted in intensity changes that were proportional to the surface slope (i.e., a linear response region).

Data were analyzed using the average values for β_0 and $d\beta/dx$ listed in Table III. Eq. (11) was used with three independent prism translation experiments at different lamp intensities to calculate the average leakage parameter Q. The nonlinear regression routine was used to determine the sample slope ψ. Results are shown in Table IV. It is seen that analysis of intensity data can be expected to yield values of the slope to an accuracy of about 0.20° for the range investigated here.

It is to be emphasized that all system calibration data necessary to determine slopes to the accuracy indicated in Table IV were obtained from prism translation experiments. The alignment procedure described in Section III and a simple calibration experiment measuring intensity as a function of prism position yield all calibration data necessary to determine slopes of tilted samples using this technique.

TABLE IV. Tilt Angles Determined by Nonlinear Regression on Intensity Data

Data Set	ψ_o, deg.	$\hat{\psi}_o$, deg.	$\psi_o - \hat{\psi}$, deg.
7901	3.422	3.337	0.085
7902	2.354	1.878	0.476
7903	1.650	1.575	0.075
7904	1.650	1.562	0.088
7905	1.129	1.177	-0.048
7906	0.7505	0.7165	0.034
7907	0.7505	0.7963	-0.4058
7908	3.0331	2.8337	0.1994
7909	3.0331	2.8826	0.1505

V. REFERENCES

1. G. Nomarski, "Differential Microinterferometer with Polarized Waves," J. Phys. Radium 16, 9S-13S (1955).

2. G. Nomarski and A. R. Weill, "Application a la metallographie des methodes interferentielles a deux ondes polarisees," Rev. Metall. 52, 121-134 (1955).

3. U. Bertocci and T. S. Noggle, "Interference Contrast Employed to Measure Slopes on Metallographic Specimens," Rev. Sci. Instrum. 37, 1750-1751 (1966).

4. Delbert L. Lessor, John S. Hartman, and Richard L. Gordon, "Quantitative Surface Topography Determination by Nomarski Reflection Microscopy. I. Theory," J. Opt. Soc. Am. 69, 357-366 (1979).

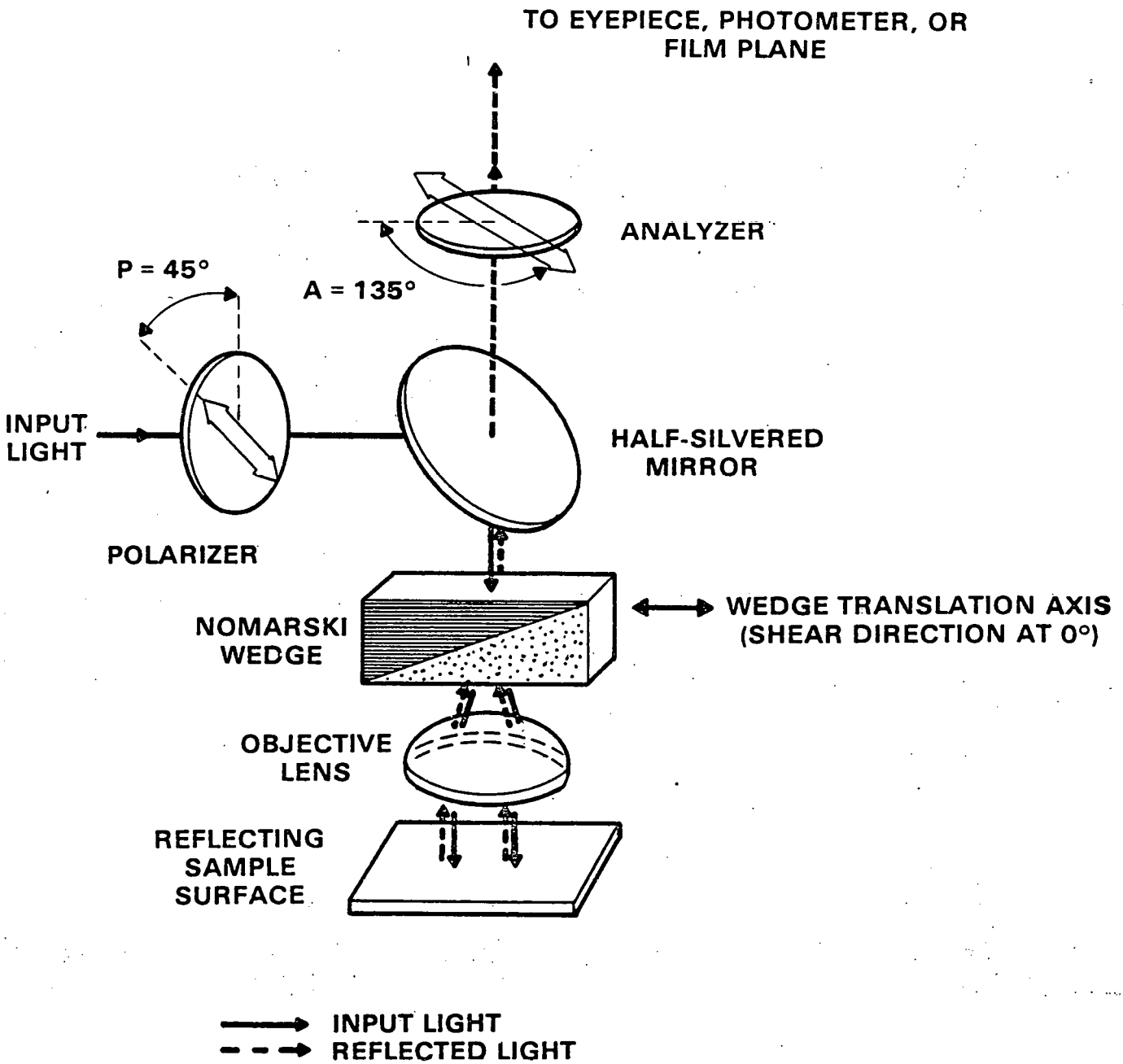

Fig. 1. Nomarski microscope system with translating wedge for phase adjustment. Angular orientation of components is measured from the Nomarski shear plane.

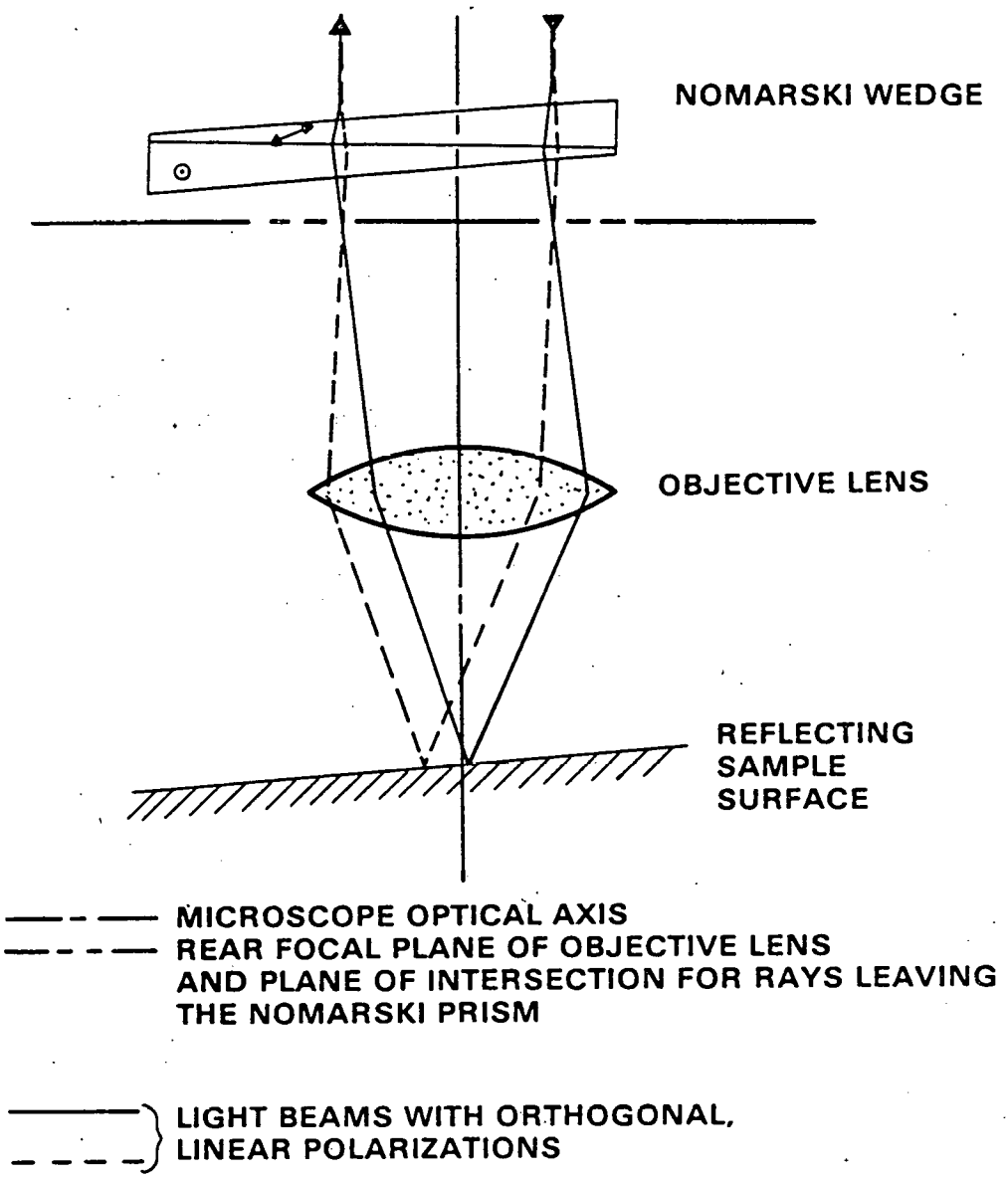

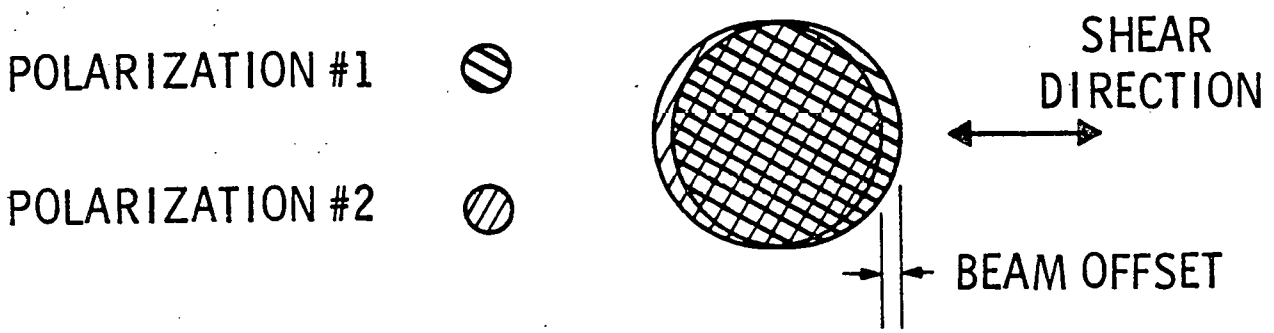

Fig. 2. Nomarski microscope schematic showing (a) the plane of apparent beam splitting and (b) the beam offset and shear direction.

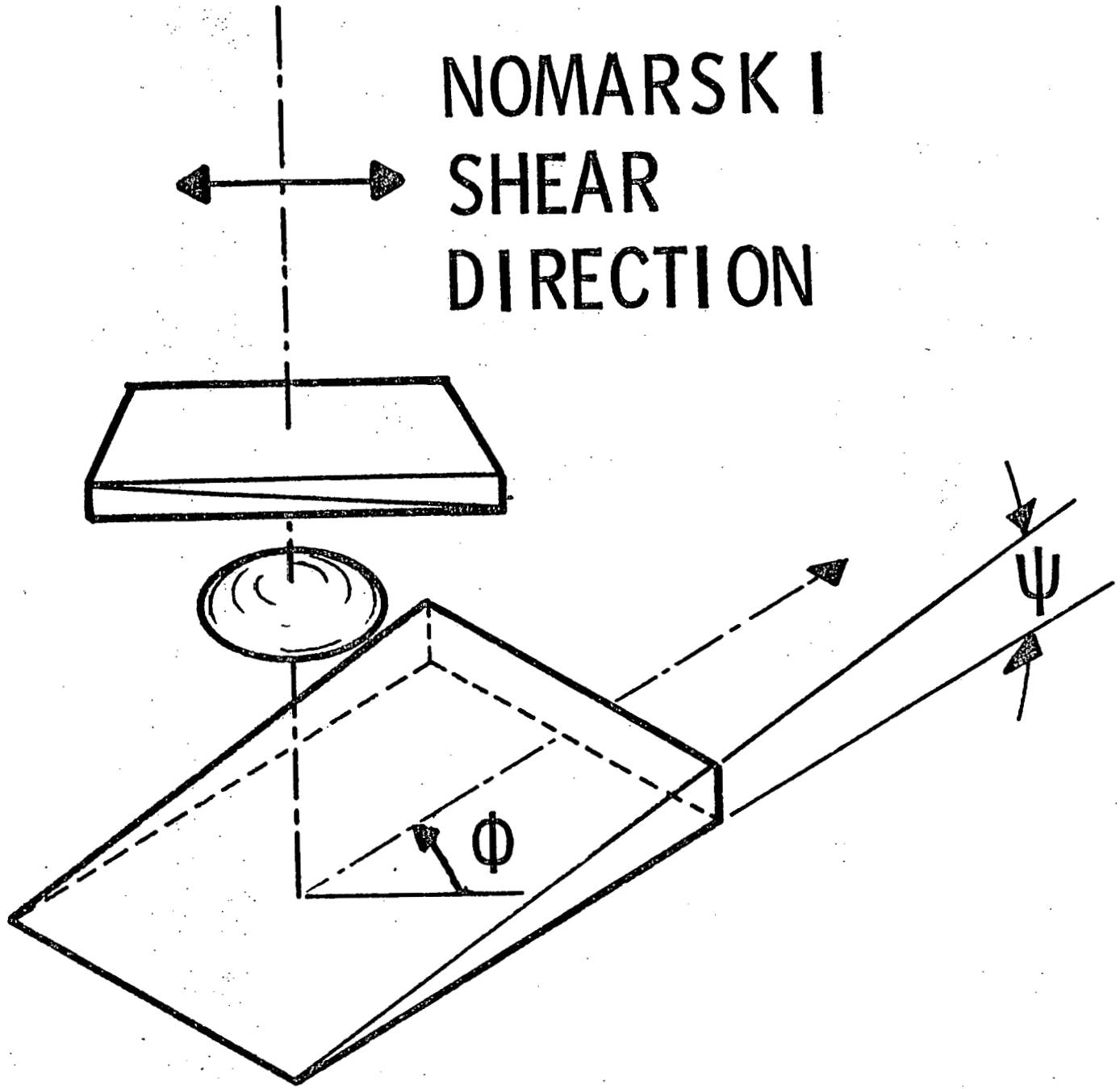

Fig. 3. Relative orientation of Nomarski prism and sample with identification of pertinent angles.

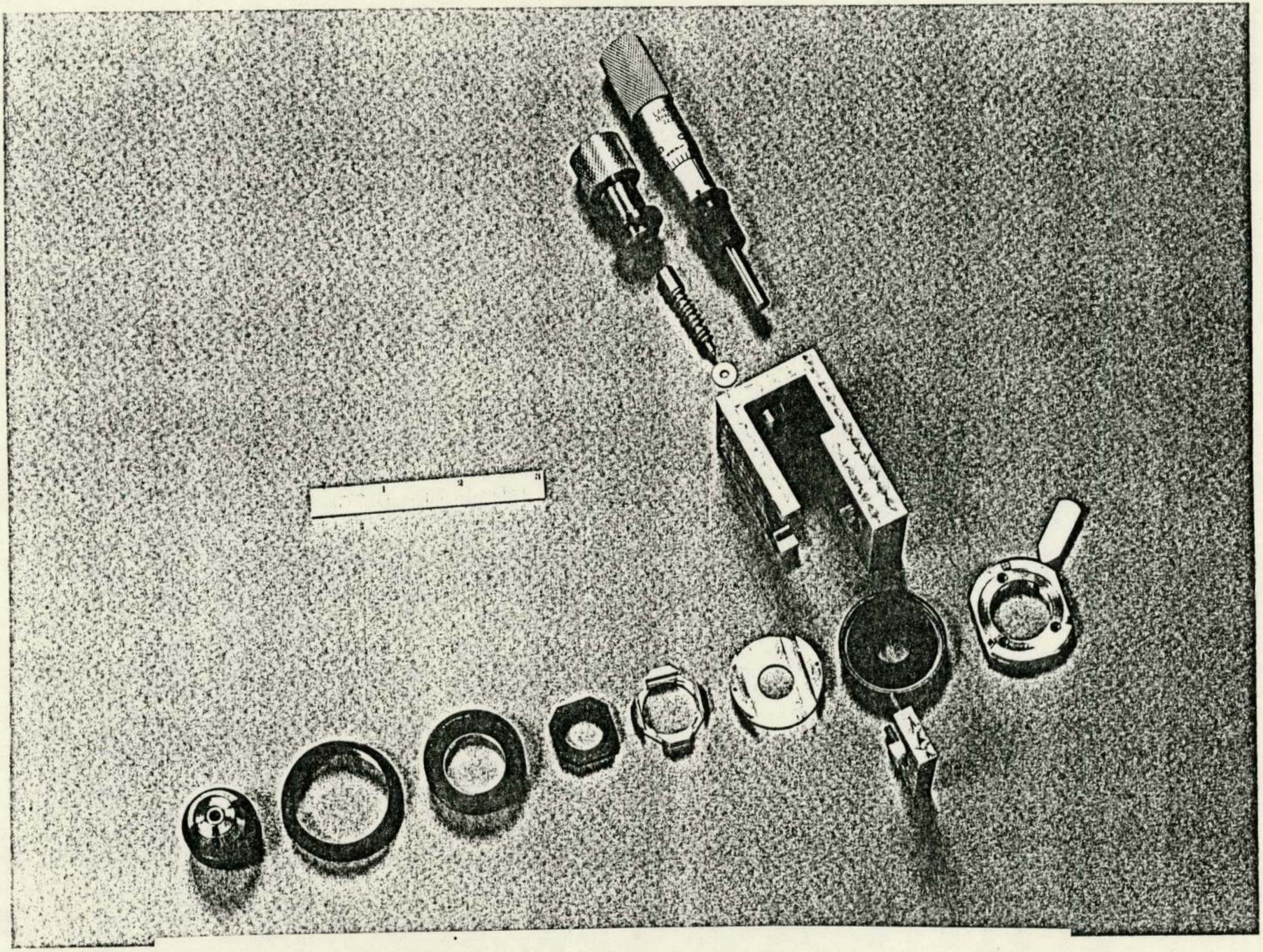

Fig. 4. Blow-up view of components used in the modified Nomarski objective assembly to provide linear motion of the Nomarski prism along its shear direction.

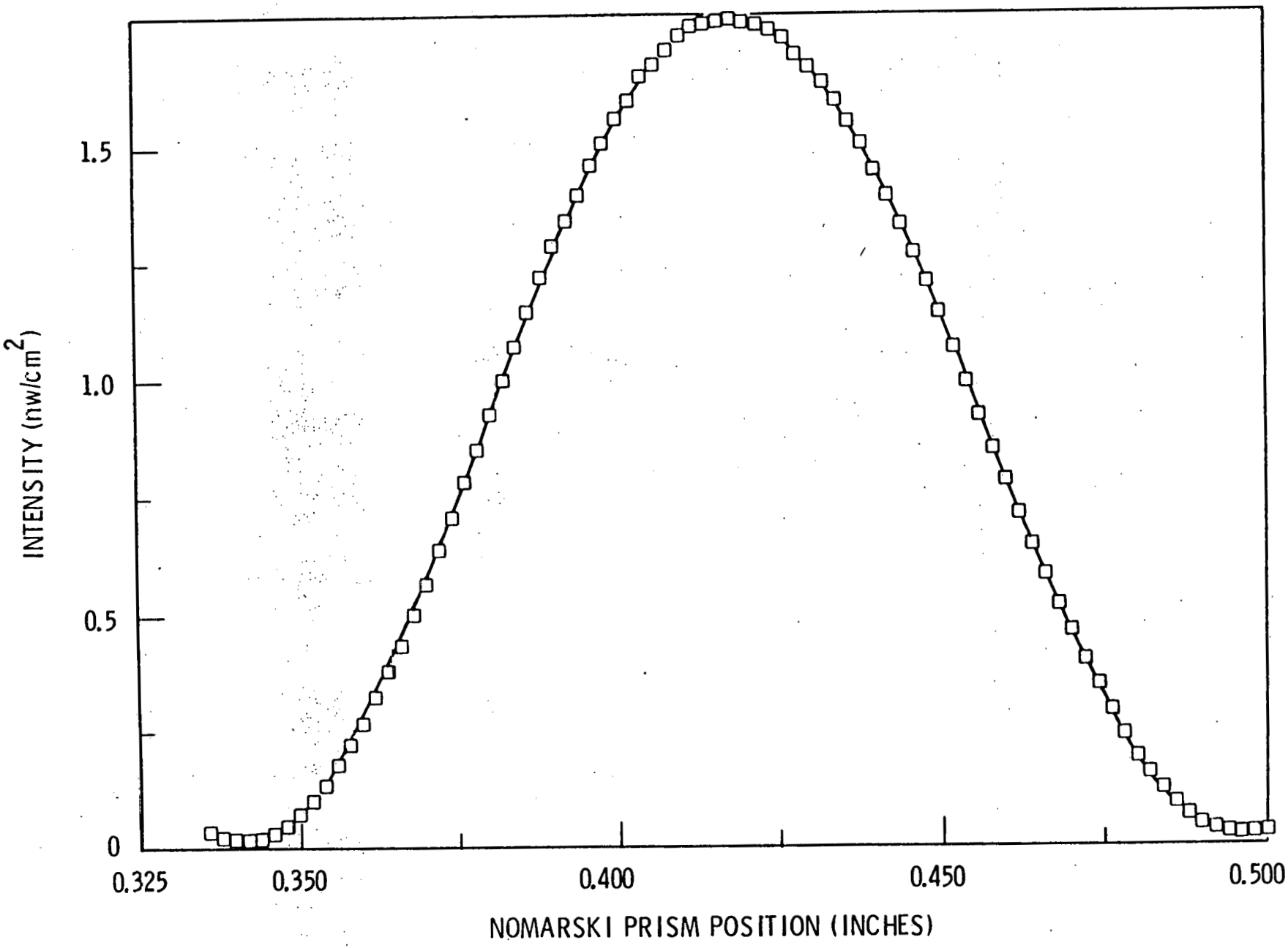

Fig. 5. Results of Nomarski prism translation experiments for a 40X objective assembly (a) intensity versus prism position with raw data (points) and non-linear regression model fit (solid line)

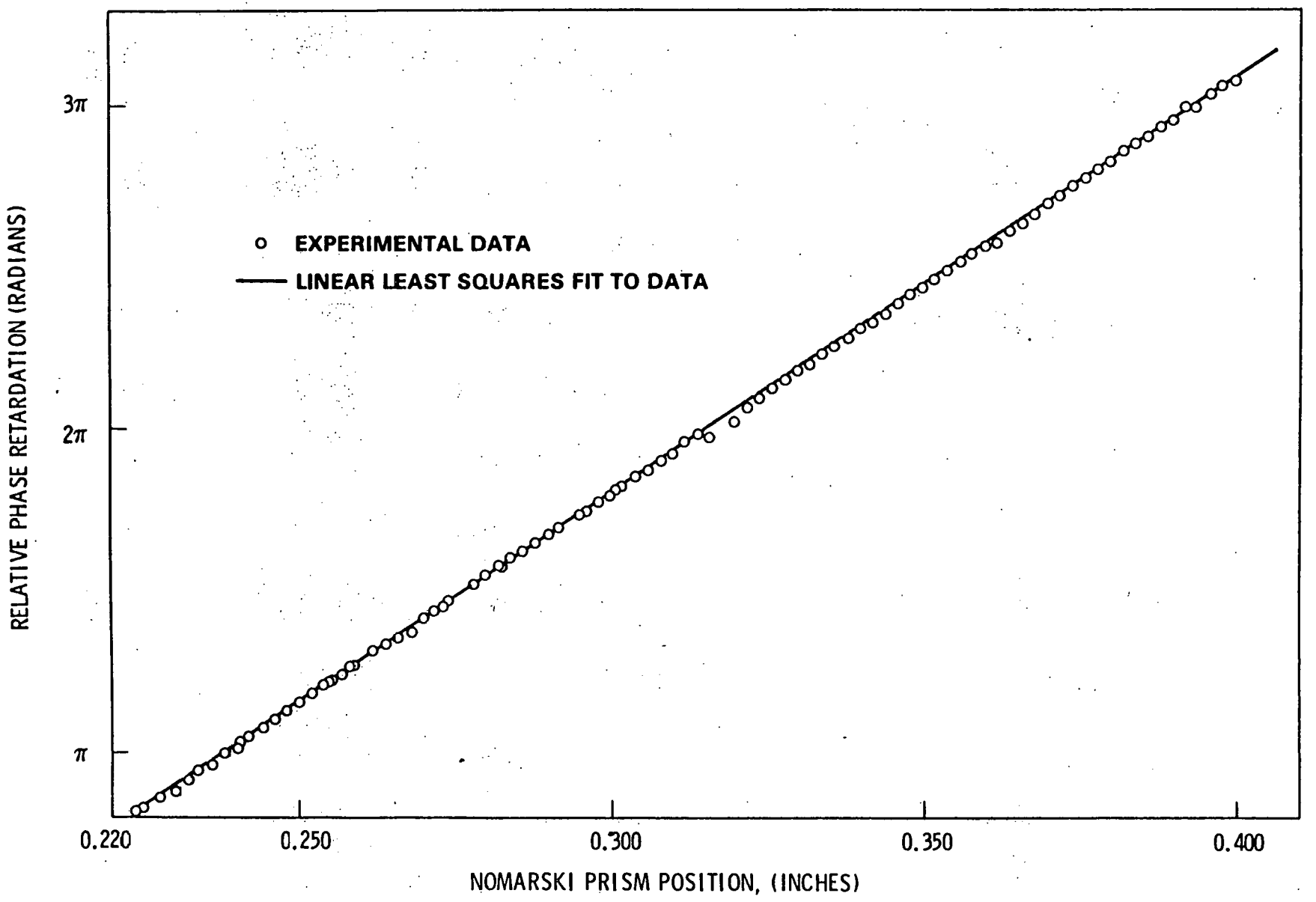

(b) relative prism phase retardation versus prism position with experimental points and linear curve fit (solid line) based on Eq. 16.

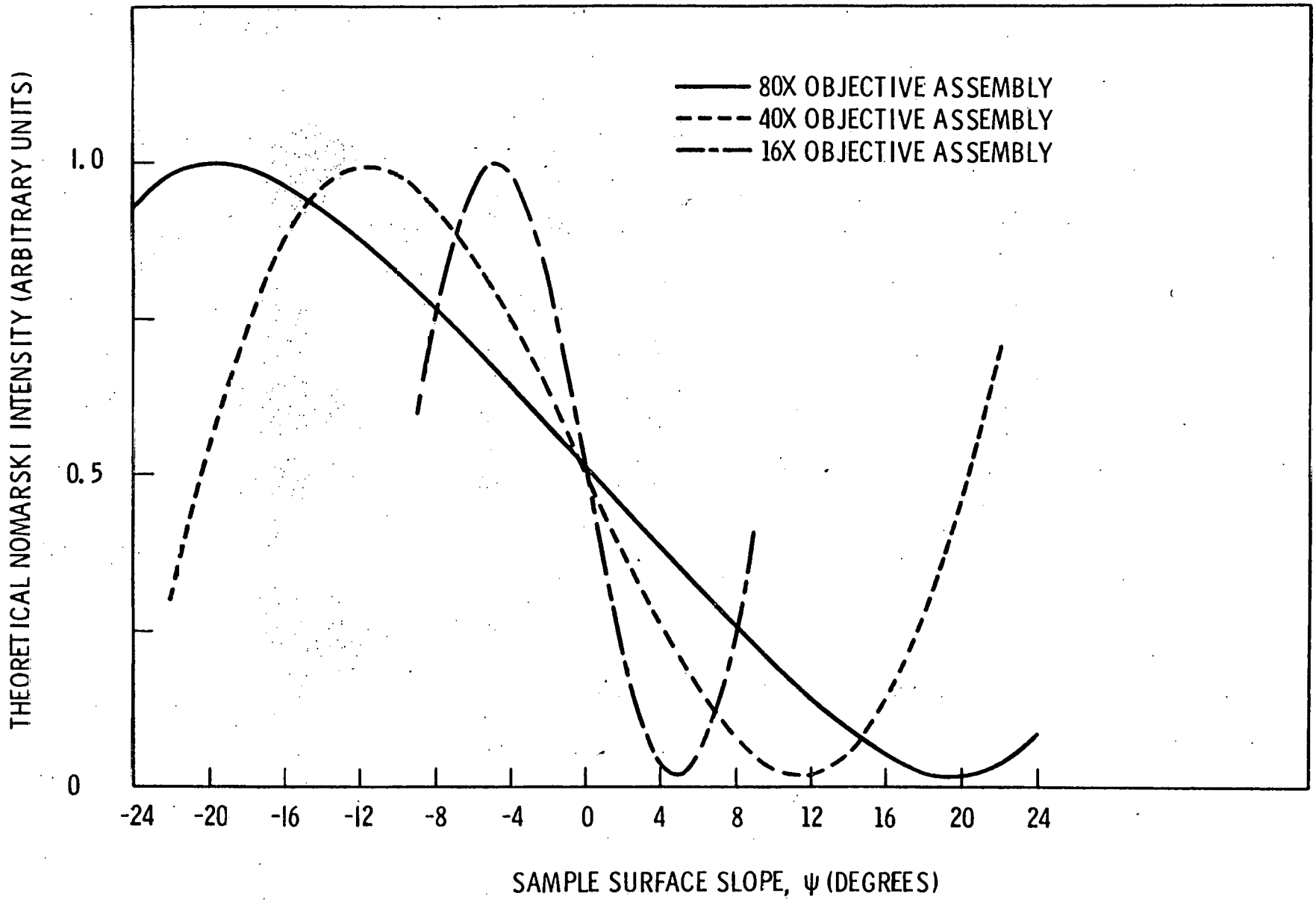

Fig. 6. Theoretical intensity dependence on sample tilt with a high conductivty sample and prism phase retardation, $\beta = \pi/2$ for selected Nomarski objective assemblies.

PAGES i to ii

WERE INTENTIONALLY

LEFT BLANK

SUMMARY

The operation of reflective Nomarski DIC microscopy for quantitative surface topography analysis has been discussed. The modification, alignment, and characterization of a commercial microscope were described to allow the adaptation of this technique to many existing microscope systems. Examples of surface slope measurements were given along with the pertinent equations used for data reduction.

THIS PAGE

WAS INTENTIONALLY

LEFT BLANK

ACKNOWLEDGMENTS

The authors wish to thank J. F. Williford for early discussions regarding the qualitative value of Nomarski DIC microscopy and to R. H. Beauchamp and D. L. Parks in whose metallography laboratory all experimental data were recorded. Special thanks also to E. V. Allen for important contributions to the design of the prism translation mechanism and for his thoroughness in performing the experiments.

This paper was prepared for the U.S. Department of Energy, Division of Basic Energy Sciences under contract EY-76-C-06-1830.